JQSRT 1906
pp: 1--20 (col.fig.: Nil)
PROD. TYPE: COM
ED: Nanda
PAGN: Vidya – SCAN: Abdul

ARTICLE IN PRESS

PERGAMON

Journal of Quantitative Spectroscopy & Radiative Transfer ▮▮▮ (▮▮▮▮) ▮▮▮–▮▮▮

Journal of Quantitative Spectroscopy & Radiative Transfer

www.elsevier.com/locate/jqsrt

Methane line parameters in HITRAN

L.R. Brown[a,*], D. Chris Benner[b], J.P. Champion[c], V.M. Devi[b], L. Fejard[c], R.R. Gamache[d], T. Gabard[c], J.C. Hilico[c], B. Lavorel[c], M. Loete[c], G.Ch. Mellau[e], A. Nikitin[f], A.S. Pine[g], A. Predoi-Cross[h], C.P. Rinsland[i], O. Robert[c], R.L. Sams[j], M.A.H. Smith[i], S.A. Tashkun[f], Vl.G. Tyuterev[k]

[a] *Jet Propulsion Laboratory, California Institute of Technology, Mailstop 183-601, 4800 Oak Grove Drive, Pasadena, CA 91109, USA*

[b] *Department of Physics, The College of William and Mary, Box 8795, Williamsburg, VA 23187-8795, USA*

[c] *Laboratoire de Physique, UMR CNRS No 5027, Université de Bourgogne, 9 Avenue A Savary, BP 47870, F-21078 Dijon, France*

[d] *University of Massachusetts Lowell, Department of Earth and Atmospheric Sciences, 1 University Ave, Lowell, MA 01854, USA*

[e] *Physikalisch-Chemisches Institut, Justus- Liebig-Universitat Giessen, Heinrich-Buff-Ring 58, D-35392 Giessen, Germany*

[f] *Russian Academy of Science, Institute of Atmospheric Optics, Laboratory of Theoretical Spectroscopy, Tomsk 634055, Russia*

[g] *Alpine Technologies, 14401 Poplar Hill Rd, Germantown, MD 20874, USA*

[h] *Physics Department, University of Ottawa, 150 Louis Pasteur, Ottawa, Canada*

[i] *Atmospheric Sciences, NASA Langley Research Center, Mail Stop 401A, Hampton, VA 23681-2199, USA*

[j] *Pacific NW National Laboratory, Richland, WA 99352, USA*

[k] *Groupe de Spectrometrie Moleculaire et Atmospherique, UMR CNRS N6089, University de Reims, UFR Sciences BP 1039-51687 Reims, Cedex 2, France*

Received 27 January 2003; received in revised form 20 March 2003; accepted 22 March 2003

Abstract

Two editions of the methane line parameters (line positions, intensities and broadening coefficients) available from *HITRAN* in 2000 and 2001 are described. In both versions, the spectral interval covered was the same (from 0.01 to 6184.5 cm^{-1}), but the database increased from 48,033 transitions in 2000 to 211,465 lines in 2001 because weaker transitions of $^{12}CH_4$ and new bands of $^{13}CH_4$ and CH_3D were included. The newer list became available in 2001 in the "Update" section of HITRAN. The sources of information are described, and the prospects for future improvements are discussed.

Keywords: Methane; Database; Line parameters; CH_3D

* Corresponding author. Tel.: +1-818-354-2940; fax: +1-818-354-5148.
E-mail address: linda.r.brown@jpl.nasa.gov (L.R. Brown).

0022-4073/03/$ - see front matter © 2003 Published by Elsevier Science Ltd.
doi:10.1016/S0022-4073(03)00155-9

1. Introduction

Spectroscopic knowledge of the methane spectrum is required for numerous remote sensing applications. Astronomical objects with detectable methane abundances typically include planets, moons and comets in our solar system. In the future, relatively cool sub-stellar objects (brown dwarfs) and planets around other stars (extrasolar planets) will be targeted for investigation [1]. The temperatures of these bodies range from less than 50 K in outer planets to over 2000 K in brown dwarfs; the required absolute accuracies of the line parameters are usually modest: 0.5 cm^{-1} for positions, 5% for intensities and 15% for broadening. Terrestrial applications generally involve a smaller temperature range (180–360 K), but the accuracies required for the spectroscopic parameters are higher (0.0002 cm^{-1} for positions, 2–3% for intensities and broadening) because observations can be taken with better signal to noise and resolution. All wavelengths from the far-infrared through the visible are potentially useful and so the ultimate goal for the database is to have a sufficiently complete and accurate representation of the methane spectrum. Because the theoretical models are difficult to implement and the spectrum is challenging to interpret, the database for methane has evolved as a mixture of theoretical predictions for the longer wavelengths and incomplete empirical results for the currently intractable regions.

1.1. The 1992, 1996, 2000 editions

In the early 1990s, available results were collected together [2] to form the 1991/1992 editions of methane line parameters consisting of line positions, line intensities, lower-state energies, air-broadening line shape coefficients (line widths, pressure-induced frequency shifts and temperature dependences of widths) and self-broadened line widths. This database appeared without significant change in the 1992, 1996 and 2000 versions of HITRAN [3–5]. The methane list consisted of (a) predicted positions and intensities for the far-infrared [6–9] and two lowest fundamentals at 7 μm (called the *dyad* polyad) [9–11] with an approximate representation of hot bands [12], (b) a mixture of calculated [13,14] and observed values [15] for the two highest fundamentals at 3.3 μm with three overtone/combination bands (*pentad*) in which the minor isotopomers were poorly represented, (c) incomplete empirical results to represent the eight-band polyad at 2.3 μm (*octad*) [2,16,17] and the 14-band polyad at 1.8 μm (*tetradecad*) [18,19]. Among the numerous deficiencies noted [2] were the dearth of experimental and theoretical results for the near-infrared and visible wavelengths, the incompleteness and inaccuracies of weak transitions, particularly for the rarer isotopomers involving vibrational levels higher than the dyad, the lack of extensive intensity and line shape measurements and the inadequacies of theoretical models to calculate pressure broadening and pressure-shift coefficients.

1.2. Progress in methane analysis

Subsequently, there was considerable progress in the analysis of the fundamental, overtone and combination bands for all three methane isotopomers including monodeuterated methane. This effort to model line positions and intensities in high-resolution spectra followed three directions.

The first one was an extension of theory to higher vibration states in order to obtain a simultaneous description of larger polyads including those with interacting vibrational states. The methane molecule has two- and three-fold degenerate vibrations, and there are coincidences between the bending frequencies $\omega_2 \sim \omega_4$, and between the stretching frequencies with their overtone/combination

states: $\omega_1 \sim \omega_3 \sim 2\omega_2 \sim \omega_2 + \omega_4 \sim 2\omega_4$. As a result of the size of these polyads, the number of ro-vibrational states and corresponding Hamiltonian terms increases very rapidly with increasing energy, thus posing a major difficulty for the accurate parameterization and prediction of the spectrum. A full account of the symmetry properties proves to be crucial for these systems.

The tetrahedral formalism [20] was successfully applied to refine the dyad [10,11] (two upper states, vibrational near-degeneracy = 5) and the pentad [21–23]: (five upper states, nine vibrational sublevels, total vibrational near-degeneracy=19). Over 4500 pentad-GS (ground state) and over 1100 pentad–dyad line positions up to J=18 were fitted with the RMS deviation of $\sim 0.001\ \mathrm{cm}^{-1}$ [21], and the RMS of 2250 fitted line intensities was $\sim 3\%$ for the pentad-GS [22]. Significant progress was also achieved for the octad [24] (8 upper states, 24 vibrational sublevels, total vibrational near-degeneracy = 55). The number of identified transitions greatly increased compared to previous isolated band analyses, although not all the bands are thoroughly assigned; the best known octad bands are at present $3\nu_4$ and $\nu_3 + \nu_4$ while the worst is $\nu_1 + \nu_2$. Some 8000 positions of the octad-GS up to J = 16 were fitted with an RMS deviation of $\sim 0.04\ \mathrm{cm}^{-1}$ and some 2500 intensities with an RMS deviation of $\sim 15\%$.

Further efforts to improve the accuracy and extend the modeling to higher J and to other vibrational states will be severely impeded by the size of the problem for the higher orders of the theory. In addition, the situation is complicated by numerous correlations (collinearity) between many of the adjusted parameters due to ambiguities of the effective Hamiltonians for degenerate and near-degenerate states [25,26]. Analysis can only be successful through a further development of the reduction theory and the availability of the right sort of experimental information for weak bands. As a result, the analysis of a higher polyad like the tetradecad at 1.6 μm is still at an early state with only 20% of the sub-vibrational levels being located [27].

The second direction was the extension of the irreducible tensor model to isotopic substitutions which change the symmetry point group $T_d \rightarrow C_{3v}$ [28]. This improved formalism, implemented in the MIRS computer package [29], permitted a more systematic treatment of various interactions at higher orders of the theory. This was subsequently applied to the simultaneous analysis of the band systems of the monodeuterated methane (CH_3D) between 3 and 11 μm [30–32]. These included the triad (three lowest fundamentals in the 900–1700 cm^{-1} region), the nonad (nine bands with 13 subbands in the region 2000–3300 cm^{-1}) and the hot band system nonad–triad (18 bands/23 identified sub-bands). In the recent study [32], nearly 10,000 line positions and 2400 line intensities were modeled with RMS values of 0.00088 cm^{-1} and 3.6%, respectively. From the theoretical point of view, this work represents the first successful achievement of the tensorial model applied to complex band systems of symmetric top molecules in which both positions and intensities could be treated in a consistent way and fitted close to the experimental accuracies.

The third effort concerns "hot band" intensity calculations that involve a plethora of overtone and combination bands arising from the dyad, pentad and octad states. However, these types of calculations most often rely on approximate extrapolations and thus require a consistent set of dipole moment parameters and wavefunctions. These in turn depend on the very accurate resonance description, and this has been achieved only for the lower polyads. Extensive experimental intensities for CH_4 hot bands are really only available for the pentad–dyad [33], and these could be fitted to 8% for 1700 lines of nine hot bands. Thus, the accuracies of these hot band calculations are in general much worse than for cold band intensities. Because of recent emphasis [1] to understand brown dwarfs and extrasolar planets, the characterization of methane difference bands now has special importance.

More information concerning the theoretical prediction, modeling and parameters of tetrahedral methane isotopic species is available at the web site http://www.u-bourgogne.fr/LPUB/shTDS.html in the form of specialized databases and software packages for spherical top molecules TDS, STDS [34,35].

1.3. Overview of the 2001 update

In Table 1, the 1992–2000 HITRAN and 2001 updates for methane parameters are summarized by giving the polyad name, the number of isotopomers, bands, range, summation of line intensities and number of lines. The line intensities and positions from 900 to 3400 cm^{-1}were replaced by new calculations based on the successful modeling of high-resolution laboratory data for all three isotopomers ($^{12}CH_4$, $^{13}CH_4$ and $^{12}CH_3D$). Hot band predictions with some empirical positions were also included for the dyad and pentad regions. In addition, a prediction of all eight bands of the main isotopomer between 3400 and 4800 cm^{-1} was merged with a collection of some 5500 empirical intensities and 10,000 line positions. Parameters below 600 cm^{-1} and above 5500 cm^{-1} were essentially unchanged, however. In Fig. 1, the $\log_{10}$ values of the line intensities from the 2001

Table 1
Comparison of 2001 and prior HITRAN methane parameters[a]

Polyad	# of Isotopes	# of Bands	Range $(cm)^{-1}$	2001 Update		1992–2000 HITRAN	
				Σ Intensity	# Lines	Σ Intensity	# Lines
Rotational	3	8	0–578	5.11×10^{-23}	8681	5.11×10^{-23}	8681
Dyad	3	27	855–2078	5.25×10^{-18}	65,478	5.30×10^{-18}	21,906
Pentad	3	34	1929–3476	1.14×10^{-17}	77,345	1.14×10^{-17}	10,184
Octad	1	9	3370–4810	9.09×10^{-19}	57,332	8.59×10^{-19}	4632
Tetradecad	2	4	4800–6185	1.22×10^{-19}	2632	1.22×10^{-19}	2632

[a] Σ Intensity values are in units of $cm^{-1}/(molecule\ cm^{-2})$ at 296 K.

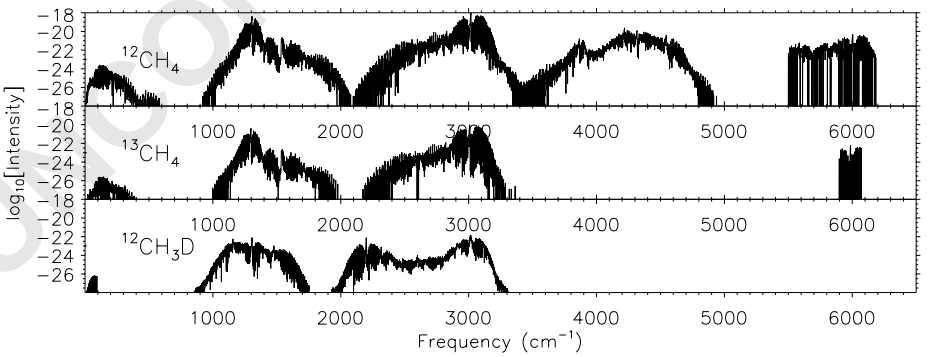

Fig. 1. The 2001 methane database for the three isotopomers ($^{12}CH_4$: top; $^{13}CH_4$: middle; $^{12}CH_3$ D: bottom). The $\log_{10}$ values of the line intensities are summed into 1 cm^{-1} bins and plotted as a function of cm^{-1}. The intensities have been scaled by the isotopic abundances.

HITRAN update are plotted as a function of cm^{-1} for each of the isotopomers. To reduce the size of the plot file, the intensities are summed into 1 cm^{-1} bins so that the maximum value on the plot does not represent the strongest individual line in the compilation but rather a sum of strongest lines of v_3. Nevertheless, the plot provides a good sense of the relative intensities of each polyad and the degree of incompleteness of the database. Above 4800 cm^{-1}, for example, there are numerous gaps in the linelist so that the trace frequently falls to zero.

In Table 2, the new collection is summarized by showing each vibrational band, the integer codes used by HITRAN for the upper and lower vibrational states, the isotopomer number (1,2,3 is $^{12}CH_4$, $^{13}CH_4$ and $^{12}CH_3D$, respectively), the number of included transitions, the wavenumber (cm^{-1}) range and the sum of the intensities. Empirical values with no assignments are listed with the vibrational code of "25 1". The number of predicted transitions in the 2001 database increased mainly because minimum intensity values for a 100% sample of the two CH_4 isotopomers were lowered to 4.0×10^{-27} $cm^{-1}/(molecule\ cm^{-2})$ at 296 K in order to provide better information for astronomical studies; The prior cutoffs ranged from 4.0×10^{-26} at longer wavelength to 4.0×10^{-24} at shorter wavelength. For CH_3D, the minimum intensity limit for a 100% sample was set to 1.0×10^{-25} $cm^{-1}/(molecule\ cm^{-2})$. For most terrestrial applications, the lower limit of 4.0×10^{-25} $cm^{-1}/(molecule\ cm^{-2})$ at 296 K is generally sufficient. Isotopomer intensities in the database were then scaled by abundances of 0.988 for $^{12}CH_4$, 0.0111 for $^{13}CH_4$ and 0.000616 for CH_3D. These scaling factors are similar to the values given in Rothman et al. [5] (0.988274, 0.0111031 and 0.000615751, respectively) but rounded to three significant digits.

In the 1992 Brown et al. paper [2], two conventions for listing quantum assignments were discussed. Below 3400 cm^{-1}, the rotational quanta were J, C (=A_1, A_2, F_1, F_2 and E) and "α", while above 3400 cm^{-1}, the quanta were J, R, C and "n". In both cases, α and n are counting integers for levels of the same J and C; the α values are incremented in order of increasing energy (see Table 6 of Ref. [2]). In the 2001 update, only the first convention (J,C, α) was used for the CH_4 rotational quantum numbers. However, the format of the database was altered to accommodate the increased range of the α from two digits to three digits. Also, the format for CH_4 is different from that of CH_3D. Examples are given in Table 3 where "mi" is the "molecule+isotopomer" code, u and l are the upper- and lower-state vibrational codes, J′ and J″ are the upper- and lower-state rotational quanta. In the newest update, the J quanta are still aligned for all three isotopomers, but the quantum number K for CH_3D is aligned with "C" of CH_4, as seen in column d.

Each transition in the database has integer codes showing the accuracy range for the line position, intensity and air-broadened width. Examples of these are shown in Table 3 in the columns labeled "*abc*" (*a* for position, *b* for intensity and *c* for air-broadened width). The precise meaning of the codes are found in Rothman et al. [3,5], but generally, accuracy values of "4" and higher represent better accuracy while "2 and 3" are well below the accuracy required for terrestrial remote sensing and even for some astronomical applications. It should be noted that for methane, these accuracy values were not generally computed from the statistics associated with the theoretical modeling. Instead, the values were set by rather arbitrary methods using the intensity of the transition. The strongest lines of the two fundamentals were given the highest rating for positions and intensities. The quality indicator was degraded according to the line intensity of the entry. For transitions involving the pentad and octad levels, some of the predicted positions were recomputed using experimental upper-state levels and so these were designated high accuracy even if the transitions had small intensities.

Table 2
Summary of 2001 methane parameters[a]

Vibration	HITRAN Codes		Iso	lines	Range		Σ Intens.
					F_{min}	F_{max}	
$^{12}CH_4$							
gs–gs	1	1	1	1747	0.010	312.781	1.98E-23
$v4$–$v4$	2	2	1	2207	2.537	367.116	2.20E-23
$v2$–$v4$	3	2	1	2297	26.675	578.722	8.70E-24
$v2$–$v2$	3	3	1	110	62.558	197.878	1.26E-26
$2v4$–$v2$	4	3	1	681	922.651	1391.509	2.39E-24
$2v4$–$v4$	4	2	1	8933	928.620	1676.111	3.76E-20
$v4$–gs	2	1	1	5303	943.985	1640.788	5.09E-18
$v2 + v4$–$v2$	6	3	1	6557	1044.045	1549.728	5.83E-21
$2v2$–$v2$	9	3	1	2230	1131.763	1753.821	1.07E-22
$v1$–$v2$	7	3	1	823	1137.534	1518.400	3.51E-23
$v2 + v4$–$v4$	6	2	1	6470	1143.389	1914.226	3.49E-22
$v3$–$v2$	8	3	1	2543	1247.021	1673.783	3.51E-22
$v2$–gs	3	1	1	3246	1302.815	1845.791	5.38E-20
$v1$–$v4$	7	2	1	697	1337.463	1844.525	2.75E-23
$2v2$–$v4$	9	2	1	1133	1380.917	2077.561	1.96E-23
$v3$–$v4$	8	2	1	5806	1411.816	2025.255	1.94E-21
$2v4$–gs	4	1	1	6700	2097.844	3229.470	5.49E-20
$3v4$–$v4$	29	2	1	482	2341.788	2775.065	2.17E-22
$v2 + 2v4$–$v2$	44	3	1	25	2452.454	2743.704	7.00E-24
$v2 + v4$–gs	6	1	1	9291	2455.981	3276.448	3.72E-19
$v1 + v4$–$v2$	10	3	1	4	2590.423	2698.736	9.23E-25
$v2 + 2v4$–$v4$	44	2	1	1821	2612.465	3156.651	1.98E-21
$v1$–gs	7	1	1	1101	2650.151	3163.633	1.67E-21
$2v2 + v4$–$v2$	45	3	1	558	2654.801	3061.949	4.10E-22
$v3 + v4$–$v2$	11	3	1	55	2668.861	2916.506	2.09E-23
$2v2$–gs	9	1	1	3590	2703.282	3476.183	3.17E-20
$v3$–gs	8	1	1	6183	2706.564	3277.552	1.08E-17
$v1 + v4$–$v4$	10	2	1	155	2798.348	3168.571	3.53E-22
$v3 + v4$–$v4$	11	2	1	3126	2828.821	3274.337	5.32E-20
$2v2 + v4$–$v4$	45	2	1	939	2835.929	3203.384	1.59E-21
$v2 + v3$–$v2$	12	3	1	2053	2836.583	3159.447	1.13E-20
$v1 + v2$–gs	46	3	1	11	2895.498	3028.013	2.68E-24
$3v3$–$v2$	47	3	1	42	2968.987	3147.017	1.28E-23
$v1 + v2$–gs	46	2	1	116	3052.686	3345.537	5.59E-23
$v2 + v3$–$v4$	12	2	1	208	3135.717	3367.367	1.09E-22
$3v2$–$v4$	47	2	1	32	3264.632	3370.087	1.04E-23
$3v3$–gs	29	1	1	8631	3354.842	4459.426	3.27E-20
$v2 + 2v4$–gs	44	1	1	11614	3712.594	4735.223	3.41E-20
unassigned	25	1	1	3274	3841.018	6184.492	7.48E-20
$v1 + v4$–gs	10	1	1	3184	3873.714	4507.039	2.53E-19
$v3 + v4$–gs	11	1	1	11247	3960.814	4608.955	4.75E-19
$2v2 + v4$–gs	45	1	1	9676	4011.160	4727.670	2.42E-20
$v1 + v2$–gs	46	1	1	2116	4226.621	4697.182	2.01E-21
$3v2$–gs	47	1	1	3071	4304.725	4938.036	1.10E-21

Table 2 (*continued*)

Vibration	HITRAN Codes		Iso	lines	Range		Σ Intens.
					F_{min}	F_{max}	
$v2+v3$–gs	12	1	1	6910	4310.318	4809.453	7.17E-20
$v3+2v4$–gs	30	1	1	11	5586.604	5624.695	1.22E-21
$2v3$–gs	13	1	1	144	5891.065	6106.284	5.97E-20
$^{13}CH_4$							
gs–gs	1	1	2	1286	0.032	309.132	2.19E-25
$v4$–$v4$	2	2	2	508	19.009	340.125	2.46E-25
$v2$–$v4$	3	2	2	446	78.511	401.385	9.39E-26
$v4$–gs	2	1	2	2895	998.884	1571.539	5.50E-20
$2v4$–$v4$	4	2	2	2754	1120.770	1484.714	4.32E-22
$v2+v4$–$v2$	6	3	2	1824	1162.140	1459.532	6.38E-23
$v1$–$v2$	7	3	2	93	1190.681	1467.342	1.71E-25
$v2+v4$–$v4$	6	2	2	853	1191.257	1720.299	3.19E-24
$v2$–gs	3	1	2	1658	1334.987	1776.976	5.23E-22
$v3$–$v2$	8	3	2	569	1347.493	1611.128	3.61E-24
$2v4$–$v2$	4	3	2	1	1368.072	1368.072	1.19E-27
$2v2$–$v2$	9	3	2	291	1398.475	1665.925	7.43E-25
$v3$–$v4$	8	2	2	1635	1471.108	1976.527	2.06E-23
$v1$–$v4$	7	2	2	84	1553.485	1685.271	1.25E-25
$2v2$–$v4$	9	2	2	44	1754.858	1953.688	7.30E-26
$2v4$–gs	4	1	2	3160	2170.216	2915.372	6.06E-22
$v2+v4$–gs	6	1	2	4962	2501.897	3209.887	4.26E-21
$v1$–gs	7	1	2	448	2702.646	3133.628	1.18E-23
$v3$–gs	8	1	2	3592	2756.028	3240.422	1.18E-19
$2v2$–gs	9	1	2	1607	2878.865	3363.229	2.39E-22
$2v3$–gs	13	1	2	83	5898.249	6069.084	5.16E-22
$^{12}CH_3D$							
gs–gs	14	14	3	80	7.760	100.026	4.24E-26
$v6$–gs	26	14	3	3788	855.753	1656.652	1.43E-21
$v3$–gs	27	14	3	1753	986.735	1698.448	1.08E-21
$v5$–gs	18	14	3	2814	1054.914	1751.856	3.49E-22
$2v6$–gs	28	14	3	4202	1929.937	3188.125	1.34E-22
$v2$–gs	16	14	3	953	1991.126	2447.965	4.88E-22
$v3+v6$–gs	34	14	3	2003	2160.454	2942.985	6.76E-24
$2v3$–gs	35	14	3	945	2337.406	3112.630	1.22E-23
$v5+v6$–gs	36	14	3	4268	2348.188	3174.778	2.31E-23
$v3+v5$–gs	37	14	3	2333	2527.403	3236.885	3.93E-23
$2v5$–gs	20	14	3	5494	2643.762	3306.810	5.99E-22
$v1$–gs	15	14	3	2327	2703.229	3252.494	3.28E-22
$v4$–gs	17	14	3	4559	2737.643	3291.875	3.97E-21

[a]HITRAN codes are the upper and lower states, respectively; 1 = the ground state (gs), 2 = v_4, 3 = v_2, etc. "v" = v. Iso is the isotope number where 1,2,3 is $^{12}CH_4$, $^{13}CH_4$ and $^{12}CH_3D$, respectively. Range is the spectral interval in cm^{-1}. Σ Intens. is in units of $cm^{-1}/(molecule\ cm^{-2})$ at 296 K.

Table 3
Sample format for the 2001 methane line parameters[a]

mi					u	l	j′ d	j″ d	*abc*
63	2919.485722	1.305E-28	0.000E+00 0.0537 0.0718	1454.56960.75 − .005614	17	14	18 6 E	1810 E	332
61	2919.498754	2.144E-25	1.320E-07 0.0510 0.0742	950.33700.65 − .005839	7	1	13F1 44	13F2 2	222
62	2919.524051	1.372E-26	5.953E-06 0.0470 0.0714	1417.19670.63 − .005839	6	1	17F2 29	16F1 2	454
63	2937.476035	2.623E-26	0.000E+00 0.0420 0.0621	1247.95590.75 − .005649	20	14	17 7 E	17 7 E	332
62	2937.483520	5.603E-22	2.253E-03 0.0630 0.0870	293.17820.73 − .006802	8	1	6F1 24	7F2 2	366
61	2937.494778	3.832E-20	2.293E-03 0.0604 0.0760	376.80480.72 − .006184	8	1	7F2 28	8F1 2	566

[a]"mi" is the molecule and isotope code where 61 = $^{12}CH_4$, 62 = $^{13}CH_4$ and 63 = CH_3D, u and l are the upper- and lower-state vibrational codes, J′ and J″ are the upper- and lower-state J quanta, respectively; d is K for CH_3 D and C for methane. "*abc*" indicates accuracy codes where "*a*" is for positions, "*b*" is for intensities and "*c*" is for air-broadened widths. For explanations of the other columns see Refs. [3–5].

Measured self- and air-broadened widths and air-broadened pressure-induced frequency shifts were inserted on a line-by-line basis for both CH_4 and CH_3D [36–52]. However, empirical pressure broadening coefficients were available for less than 2% of the 211,465 methane transitions (as described in the next section). For the unmeasured majority of the transitions, the crude scheme of estimated values from Ref. [2] was generally used for air- and self-broadened widths. The accuracy of these estimates were thought to be no better than 20% and were given an accuracy code of "2 or 3". When individual measurements were inserted, the accuracy codes were entered as "5 or 6" indicating 5–2% uncertainties.

In the prior database [2], the temperature dependence of the widths "*n*" was set to 0.75 for all lines. For the 2001 update, the temperature dependence of the air-broadened widths were estimated values obtained from averaging empirical values [39,43] according to *m*, where *m* = lower state J for P and Q branch and upper state J for R branch transitions. These are shown in Table 4. Uncertainties of these averages are assumed to be ±40%. The values in the column "n_{dyad}" are solely averages by "*m*" of new measurements from the dyad [39], but these were inserted for the rest of the parameters in the dyad and pentad. The values in column "n_{octad}" were based on measurements [43] in the three strongest octad bands and were applied only to that region.

Air-broadened pressure-induced shifts in cm^{-1} atm^{-1} were computed as a function of the line position v_i to estimate crudely the change of the shifts as a function of the vibrational quanta.

$$\text{shift} = -0.002v_i/1300 \quad \text{for dyad,}$$

$$\text{shift} = -0.006v_i/3000 \quad \text{for pentad,}$$

$$\text{shift} = -0.008v_i/4400 \quad \text{for octad,}$$

$$\text{shift} = -0.008 \quad \text{for tetradecad.}$$

These shift values could be wrong by a factor of two in some cases.

For CH_3D, empirical expressions obtained from some 1300 measurements of the three lowest fundamentals [46–51] were used to calculate the air- and self-broadened widths of some 25,000

Table 4
Temperature dependence (n) for CH_4[a]

m	n_{dyad}	n_{octad}
1	0.63	0.65
2	0.65	0.68
3	0.80	0.70
4	0.80	0.73
5	0.75	0.72
6	0.72	0.72
7	0.73	0.70
8	0.72	0.70
9	0.67	0.69
10	0.67	0.65
11	0.65	0.64
12	0.65	0.64
13	0.65	0.63
14	0.65	0.63
15	0.65	0.62
16	0.63	0.62
17	0.63	0.61
18	0.63	0.61
19	0.63	0.60
20	0.63	0.60
21	0.61	0.59
22	0.61	0.59
23	0.61	0.58
24	0.61	0.57
25	0.61	0.57

[a]m is J″ for P and Q branch lines and J″ + 1 for the R branch. n_{octad} values are from Ref. [43]; n_{dyad} values are from Ref. [39]. The uncertainties of the averaged values are assumed to be ±40%.

unmeasured transitions. The data analyzed included values of J up to 18 and values of K up to 15. For most transitions, the expression used was

$$\text{width}_{air} = 0.0677 - 5.681 \times 10^{-5} m - 8.397 \times 10^{-5} k^2,$$

$$\text{width}_{self} = 0.0869 - 6.41 \times 10^{-5} m - 6.56 \times 10^{-5} k^2,$$

where m is as described above, and k = lower state K for $\Delta K = -1$ and 0 and k = upper state K for $\Delta K = +1$.

In the analysis, it was found that a different expression was required for transitions with $J'' = K''$ for PP, QQ, RR lines

$$\text{width}_{air} = 0.06863 - 3.762 \times 10^{-4} m + 7.044 \times 10^{-7} m^2,$$

$$\text{width}_{self} = 0.0875 - 3.46 \times 10^{-4} m + 4.94 \times 10^{-7} m^2.$$

For all unmeasured CH_3D transitions, the air-shift $= -0.0025 v_i/1300$, and the temperature dependence of the air-broadened widths was defaulted to a constant of 0.75.

Although the air- and self-broadened CH_3D widths were measured with 3% uncertainty [46–51], these data could be reproduced by the empirical expressions to only 6–7%. Thus, the transitions in the new database between 2000 and 3300 cm^{-1} have less accurate widths than those transitions of the triad (from 1000 to 1700 cm^{-1}) for which the widths are replaced by empirical values. As with any polynomial expansion, the computed values at higher J and K become very unreliable; for example, if computed widths were negative, they were reset to 0.02 cm^{-1} atm^{-1}. Even so, these estimated values of CH_3D widths are thought to be more accurate (±7%) than the estimated CH_4 widths (±20%) in Ref. [2].

In the remaining sections, the parameters in each spectral region and the prospects for future improvements are discussed. The reader is directed to the individual publications for complete details.

2. Database for the methane polyads

2.1. Rotational region: 0.01–579 cm^{-1}

The 2001 methane list in this region is the same as the 1992–2000 versions. The database contains transitions arising between ground–state levels of the three isotopomers and hot bands arising from v_4 and v_2 levels ($v_4 - v_4$, $v_2 - v_2$ and $v_2 - v_4$) for both $^{12}CH_4$ and $^{13}CH_4$ [6–9]. The positions of the difference bands were predicted from ro-vibrational analysis of the two lowest fundamentals [10] that achieved a standard deviation of 0.00008 cm^{-1}. The methane intensities were calculated from a theoretical extrapolation based on the dyad analyses; the accuracies were thought to be no better than 30%. The self- and air-broadened widths and the temperature dependence coefficients were unchanged from the estimated values listed in Ref. [2].

2.2. Dyad: 855–2080 cm^{-1}

As indicated previously, the 1992, 1996 and 2000 versions of the HITRAN database [3–5] contained predictions of v_4 at 1310 cm^{-1} and v_2 at 1533 cm^{-1} for both $^{12}CH_4$ and $^{13}CH_4$ [10,11], as well as an approximate prediction for nine hot bands of $^{12}CH_4$ [12] arising from the dyad to the pentad upper-state levels. For the updated version in 2001, a comprehensive analysis [33] provided improved predictions of the 10 pentad–dyad hot bands of both $^{12}CH_4$ and $^{13}CH_4$; the dyads of both these species were refitted as well. The number of transitions in this region increased from 21,906 to 65,478 because the minimum intensity cutoff was lowered to 1×10^{-27} $cm^{-1}/(molecule\ cm^{-2})$ at 296 K. The integrated intensities for this region (shown in Table 1) decreased 1% because of adjustments to some of the band intensities.

The rms of the fitted dyad positions was 0.00008 cm^{-1} for low to moderate J. The accuracies of the hot band positions were worse because of the less accurate modeling of the pentad levels [12]. To improve the accuracies, many of the positions were recomputed using empirical upper-state levels; the accuracy codes indicate which have been altered. The uncertainties of the intensities are thought to be 3% for the strong dyad lines and 6–20% for the hot bands. Prior measurements of several hundred pressure broadening coefficients for $^{12}CH_4$ and $^{13}CH_4$ [36–39] were merged with estimated values of air- and self-widths in Ref. [2] and temperature dependence of widths based on averaging measurements by J or m, as shown in Table 4.

The dyad region of methane contains bands of the $^{12}CH_3D$ triad consisting of ν_6 near 1161 cm^{-1}, ν_3 near 1307 cm^{-1} and ν_5 near 1472 cm^{-1}. The 1992, 1996 and 2000 editions contained calculations of the positions and intensities based on earlier work [53]. In 2001, these were replaced by preliminary predictions [31,32]. Ultimately, using new ground-state constants [54], 3467 positions were modeled to 0.0005 cm^{-1} and some 800 intensities to 2.2% [32,55]. An analysis of $^{13}CH_3D$ positions was published [56], but no prediction was made available from this study. The nonad–triad hot bands of $^{12}CH_3D$ were not included in the 2001 updated database, but some of these will likely be available in the future.

For CH_3D line widths, an extensive new set of measurements [46–51] permitted over 1300 empirical values for the air- and self-broadened widths and shifts to be inserted line-by-line into the updated 2001 version of the database. The accuracies of the measured widths and shifts are thought to be 3% and 0.0003 cm^{-1} atm^{-1} or better, respectively.

2.3. Pentad: 1980–3450 cm^{-1}

Before 2001, the methane database in this region consisted of a semi-empirical list from the 1986 edition of HITRAN [57] that was based on less accurate modeling [13,14] of positions and intensities (many of which were from hand-measured grating spectra [15]). In all prior versions of HITRAN, discernible features that coincided with expected assignments were marked as $^{13}CH_4$ and $^{12}CH_3D$; many transitions of these isotopomers were missing or inaccurately represented. In addition, numerous entries were given with no assignment, although empirical ground states [15] were listed for some.

In 2001, this motley collection of line parameters was totally replaced by a set of new calculations for all three isotopomers, increasing the number of lines from over 10,184 to over 77,345. Predictions of pentad bands, ν_1, ν_3, $2\nu_4$, $2\nu_2$ and $\nu_2+\nu_4$, for $^{12}CH_4$ and $^{13}CH_4$ were based on the several new studies [21–23]. The accuracies were 0.001 cm^{-1} and 3%, respectively, for the positions and intensities from the theoretical modeling. Preliminary predictions of 14 hot bands of $^{12}CH_4$ for the tetradecad–dyad were also added [27,35], but no analysis of the $^{13}CH_4$ tetradecad was available to characterize the corresponding hot bands of the second isotopomer. The estimated hot band accuracies are 0.04–1 cm^{-1} for the calculated positions and from 20% to factors of five for the calculated intensities. Some of the line positions in the $^{12}CH_4$ hot band predictions were recomputed with experimental upper-state values [27] in hopes of obtaining an accuracy of 0.001 cm^{-1}. The estimated values for pressure broadening described in the introduction were used for most of the CH_4 transitions. Some 1000 individual measurements of air-broadened line widths and shifts were inserted on a line-by-line basis from the 1992 database and from recent published results [40–42]. In addition, preliminary unpublished values [52] for some 478 features from 2600 to 3156.6 cm^{-1} were added. The accuracy codes serve to flag those entries with experimental rather than estimated values.

A significant improvement was made for the $^{12}CH_3D$ parameters in the pentad region. For the new database, predictions of the nine bands of the nonad (ν_1, ν_2, ν_4, $2\nu_6$, $2\nu_3$, $2\nu_5$, $\nu_3+\nu_6$, $\nu_3+\nu_5$ and $\nu_5+\nu_6$) from 2000 to 3200 cm^{-1} were generated [31,32]. The accuracies of the positions and intensities are thought to be 0.0009 cm^{-1} and 4%, respectively, based on the modeling of 6796 positions and 2459 intensities. For the line widths, the empirical expressions for the self- and air-broadened widths and estimated values of shifts and temperature dependences (described previously) were used.

2.4. Octad: 3370–4810 cm^{-1}

Prior to 2001, the database consisted of an empirical linelist of some 4632 positions and intensities between 3700 and 4665 cm^{-1} [2]. Probable quantum assignments based on combination differences for four bands were listed for one-third of the features, and empirical lower states were given for some 2000 entries below 4170 cm^{-1}.

In 2001, these parameters were replaced by a $^{12}CH_4$ prediction [24] with over 57,000 lines belonging to eight bands: $3\nu_4$, $\nu_2+2\nu_4$, $\nu_1+\nu_4$, $\nu_3+\nu_4$, $2\nu_2+\nu_4$, $\nu_1+\nu_2$, $\nu_2+\nu_3$ and $3\nu_2$. The modeling was sufficient to reproduce nearly 8000 positions up to J = 16 with an RMS of 0.041 cm^{-1} and 2500 intensities up to $J = 14$–16%. The positions and intensities of the strongest transitions in the prediction were then replaced with existing empirical values ([2–4] and the references therein) and new measurements [45]. As for the longer wavelengths, the accuracy codes can be used to discern which values were replaced with the older measurements. In Fig. 2, synthetic spectra are shown for the 4550–4590 cm^{-1} region of $\nu_2+\nu_3$ and $3\nu_2$. The assumed pressure, temperature and path values are 38 Torr of normal sample methane, 296 K and 20 m, respectively. The top plot is computed using the 1992–2000 HITRAN with 12 features, and the bottom is computed using the 2001 methane database with 1925 transitions. The vertical lines at the top of each plot indicate the positions of individual lines in the lists. Lines weaker than 1×10^{-23} $cm^{-1}/(molecule\ cm^{-2})$ at 296 K that were totally missing from the prior versions of the database [3–5] are now represented through the prediction, but they could have larger uncertainties of 15%–50% for intensities and 0.1–1.0 cm^{-1} for positions.

Some observed features are given with no assignment. All these entries are taken from the new measurements [45]. As seen in Fig. 1, no transitions of $^{13}CH_4$ and $^{12}CH_3D$ are included in the octad region, although a few of the unidentified features may in fact be $^{13}CH_4$.

For terrestrial applications, only the stronger transitions are needed. However, the linelist for the octad region is still incomplete for the studies of outer planets with higher abundances of methane. For brown dwarfs with higher temperatures, higher J lines are required along with hot bands arising from the dyad, pentad and octad as the lower states.

Pressure-broadening information for this interval comes from the estimated values in Ref. [2] and Table 4, combined with empirical results including temperature-dependence coefficients for the three strongest bands $\nu_1+\nu_4$, $\nu_3+\nu_4$ and $\nu_2+\nu_3$ [43,44]. To satisfy the needs of the MOPITT [58] application, over 1000 new room-temperature broadening widths and shifts [45] were inserted between 4260–4305 and 4350–4500 cm^{-1}. This new investigation utilized higher optical densities than prior studies [43,44] so that air-broadening parameters of weaker bands and higher J of the stronger bands were measured. The study also obtained for the first time an extensive set of self-broadened widths and shifts, increasing the number of available measured self-broadened widths [36,41] by a factor of 10. The systematic variation of the observed values as a function of rotational quanta will be described in a publication [45]. It is hoped that ultimately this extensive empirical dataset, involving several different combination bands, will lead to improved theoretical predictions of methane line shape parameters.

2.5. Tetradecad: 4800–6250 cm^{-1}

Fourteen bands (ν_4, $\nu_2+3\nu_4$, $\nu_1+2\nu_4$, $\nu_3+2\nu_4$, $2\nu_2+2\nu_4$, $\nu_1+\nu_2+\nu_4$, $2\nu_1$, $\nu_1+\nu_3$, $\nu_2+\nu_3+\nu_4$, $3\nu_2+\nu_4$, $\nu_1+2\nu_2$, $2\nu_3$, $2\nu_2+\nu_3$ and $4\nu_2$) give rise to transitions from the ground state in this

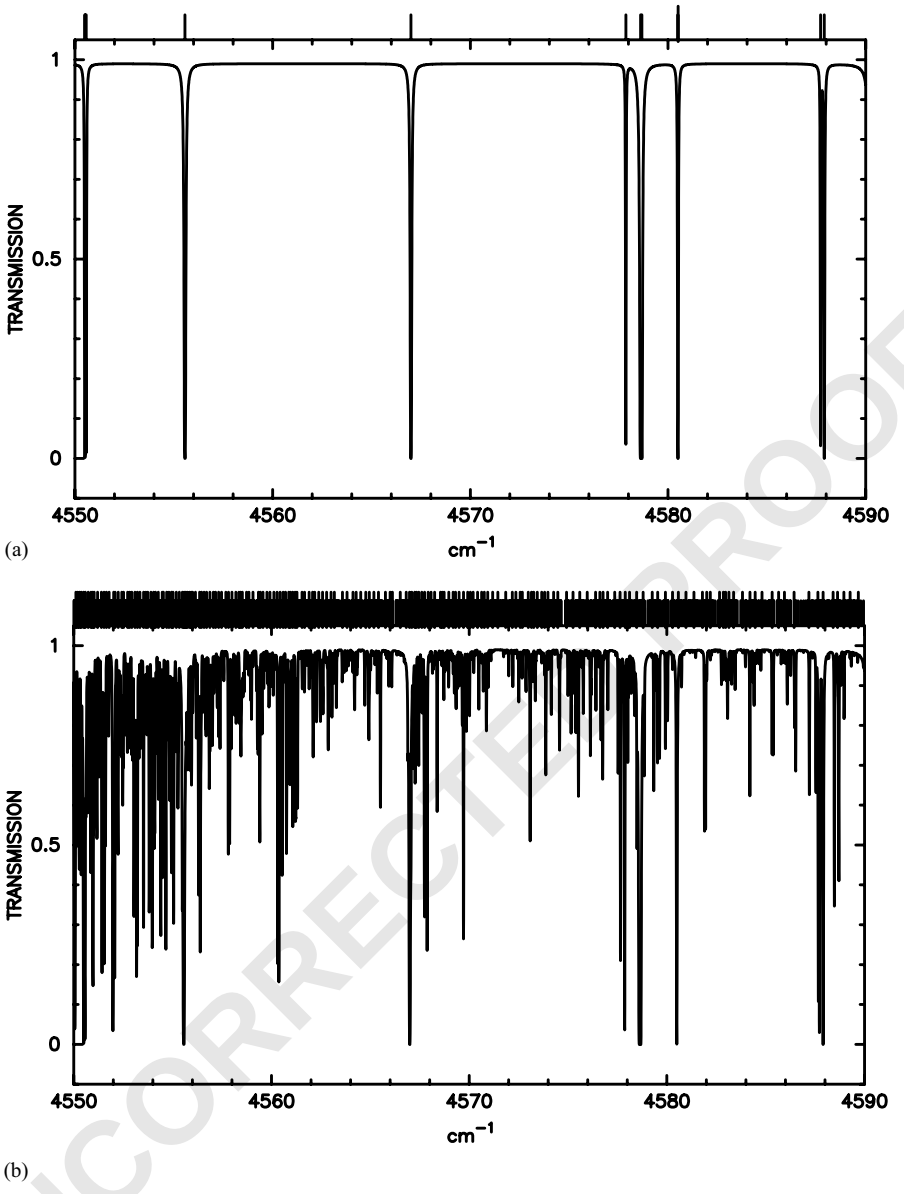

Fig. 2. Comparison of calculated spectra using two methane databases. The assumed optical density is 1.0 m atm at 296 K (20 m and 38 Torr of normal methane), and the resolution is 0.01 cm^{-1}. The upper and lower traces are based on the 1992–2000 HITRAN and the 2001 updated version, respectively. Vertical lines indicate positions of transitions used. The upper panel has 12 features measured empirically while the lower panel has 1925 mostly predicted transitions.

region [27], but the theoretical modeling was not sufficiently reliable to warrant replacement of the parameters in 2001. The linelist for this spectral region therefore has not been changed since 1992. It covers only the 5500–6184.5 cm^{-1} interval and is based on the empirical measurements [18,19] for

2632 line positions and intensities; many empirical lower-state energies were obtained by measuring intensities at different temperatures [19]. Estimated broadening coefficients are determined from the 240 assignments of $^{12}CH_4$ and $^{13}CH_4$ allowed lines of $2\nu_3$ and $\nu_3+2\nu_4$ or by estimating "m" to be the lower-state J″ obtained from the experimental lower-state energy, where $E'' \approx BJ(J+1)$ and the rotational constant B is 5.2 cm^{-1}. However, all the air-broadened pressure shifts are set to a constant value of -0.008 cm^{-1} atm^{-1}. Additional details about the formation of this section of the database are given in [2].

3. Prospects for future improvements

In Table 7 of Ref. [2], 10 deficiencies in the 1992 database were listed. The 2001 methane compilation incorporates changes to address five that involve transitions between 900 and 4800 cm^{-1}. The remaining deficiencies concern the dearth of accurate intensity measurements in the far-infrared, the lack of theoretical models for the near-infrared and the slow progress in quantifying the line shape parameters to the accuracies required.

3.1. near- and far-infrared bands

Experimental and theoretical work in progress gives some hope that more improvements can be made in the coming years. The astronomical applications have long needed better parameters for the near-infrared wavelengths; those investigations have relied on low-resolution (10 cm^{-1}) information such as band model representations [see [59] and the references therein] from 2000 to 9500 cm^{-1}or absorption coefficients from 4000 to 6000 cm^{-1} (see Ref. [60]). For the shorter wavelengths, empirical absorption coefficients at 1 cm^{-1} resolution are available [61] from 10,635 to 13,300 cm^{-1}. However, new efforts now in progress will provide initial results at high resolution. For example, an empirical list of nearly 40,000 line positions and intensities at room temperature has been obtained at 0.01 and 0.02 cm^{-1} resolution [62] using the Fourier transform spectrometer located at Kitt Peak; the average accuracies are 0.005 cm^{-1} for positions and 15% for intensities from 4800 to 5500 cm^{-1} and from 6180 to 10,000 cm^{-1}; three intervals (4800–5500 cm^{-1}, 7400–7650 cm^{-1} and 8950–9150 cm^{-1}) are being measured with better accuracies. Transition identifications for the strongest bands near 6000 cm^{-1} [27], 7500 cm^{-1} [63], and 9000 cm^{-1} [64] will be included in the new list, but in fact, the quantum assignments of very few of these features are known. An empirical list of methane features has also been obtained from hot methane up to 1273 K [65]. These data potentially can facilitate ab initio investigations [66–68] to predict all possible methane bands up to the visible wavelengths.

Model predictions are usually desired over empirical lists. As demonstrated in Fig. 2, the weaker features are quite abundant and require time-consuming efforts to measure and catalog. Stronger transitions mask the presence of the weaker entries, and blending degrades the experimental precisions. In the interim, the experimental linelists, despite their inaccuracies and incompleteness, can serve as a reference list for applications involving modest abundances of methane near room temperature and also for future theoretical analysis of laboratory data. However, for the extremely cold and extremely hot environments, only successful modeling can produce the required parameters.

Unfortunately, minimal progress is being made to address other deficiencies. Only a few far-infrared line intensities [69] have been attempted. No studies for the minor isotopomers are in progress or even expected for the octad and tetradecad regions.

3.2. Line shape refinements

The basic pressure broadening measurements have not been done for the near-infrared bands nor for the weaker lines in the fundamental regions, nor are there extensive measurements of the temperature dependence of the broadening coefficients. The available measurements of Voigt and Lorentz profiles involve the strongest (allowed) transitions, and these have not resulted in a reliable methodology to transfer measured broadening coefficients in the lower polyads to unmeasured transitions in other polyads, as is possible with species such as water [70]. Theoretical models for widths have not yet reproduced the measurements to within experimental accuracies (3%). Moreover, a recent investigation [71] indicates that different types of line shape coefficients are needed for the terrestrial applications.

The spectroscopic parameters tabulated in HITRAN are intended to calculate only additive Lorentz or Voigt profiles for each transition. However, there are a number of collision phenomena that may significantly distort these profiles under typical atmospheric conditions. These effects include Dicke narrowing [72–75], speed-dependent broadening and shifting [76,77], and line mixing [78–83]. Since these mechanisms often occur together, a number of generalized profiles have been presented recently combining Dicke narrowing with speed dependence [84–88], Dicke narrowing with line mixing [89] and all three [90]. Each of these line shape anomalies have been observed for methane [41,71,91–95].

Dicke narrowing results from a constriction of the inhomogeneous Doppler distribution due to velocity-changing collisions responsible for mass diffusion [72–75]. It is most apparent at low-to-moderate pressures as is found in the upper atmosphere [41,92], yielding deviations from the Voigt profile of a few percent near line center. The relationship of the velocity-changing collision rate to the macroscopic diffusion constant is only approximate [41] and may require an extra parameter for each transition [92,94,95].

Speed-dependent broadening and shifting is a consequence of the finite range of the intermolecular potential yielding a collision cross section that depends on the relative kinetic energy [76,77]. It affects the line profile at pressures throughout the atmosphere and is difficult to distinguish from Dicke narrowing at lower pressures. However, it persists at higher pressures where it has been observed to yield spectral deviations on the order of 1% in the P and R branches of the v_3 band of methane [94]. A comparable study of the Q branch exhibited no speed-dependent spectral signatures [95]. Currently, there are no theoretical calculations of the kinetic-energy dependence of the collision cross sections available for methane from which we may estimate the speed dependence from a realistic potential.

Line mixing is an interference between overlapped transitions coupled by rotationally inelastic collisions [78–83]. For the complex methane spectrum, it causes deviations up to tens of percent from linearly superimposed profiles at higher pressures, representative of the troposphere [41,71,91–95]. If the overlap and coupling are weak, line mixing can be treated as a first-order dispersive correction [83,91,92,94,95] for each transition with one extra parameter per line. However, in case of strong overlap and coupling, a more complete description of the "relaxation" matrix is required, along with a numerically intensive inversion procedure [71,78,93–95]. The relaxation matrix consists of the

broadening and pressure shift coefficients on the diagonal and the line couplings as the off-diagonal elements. Generally, there are too many couplings to be determined empirically; so theoretical models are usually invoked. For methane, a semi-classical calculation of rotational state-to-state collision rates has been scaled to fit the spectral data [71,93–95] with moderate success.

Ideally, the line shape coefficients that include other types of effects are to be calculated as a function of the quantum numbers using models verified by measurements. There has been some effort to predict Lorentz parameters [96] that gave an absolute average difference of 6% compared with limited ν_3 measurements. There are now more extensive datasets for methane [36–45] and monodeurated methane [46–51] for testing and refining theoretical models. Nevertheless, the laboratory data are still insufficient to satisfy remote sensing requirements at all wavelengths; new air- (terrestrial) or Hydrogen- (planetary) broadening measurements are needed to investigate the vibrational dependence of the Lorentz and non-Lorentz profiles. For laboratory studies, the allowed lines of the two infrared fundamentals are the most accessible, but these lines are saturated for many applications and so it will be necessary to characterize these effects for several thousand weaker transitions in the fundamental regions and in the higher polyads (such as $2\nu_3$). The lack of accurate air-broadening coefficients is already hindering ongoing remote sensing experiments from the dyad region at 8 μm [97] to the tetradecad region at 1.6 μm [98].

4. Conclusions

The 2001 compilation of methane parameters represents the collection of results available up to December of 2000. The major enhancements involve the pentad and octad polyads of the main isotopomer and the fundamental regions of the other minor species.

In the last decade, there has been significant progress in understanding and predicting the spectrum of methane in the lower polyad regions, but many improvements are still needed, particularly for the near-infrared. Line shape measurements and modeling are increasingly important.

The future challenge will be to bring different types of spectral information for a wide range of applications into a common form for future database updates. The 1992 paper [2] noted that the number of groups studying methane had decreased, and this situation has not improved in the interim. As a result, future advancements are likely to occur very slowly.

Acknowledgements

The authors thank J. Brault, C. Plymate and M. Dulick at the National Solar Observatory for assistance in recording the methane spectra. We also thank G. Toon for his assistance with graphics and D. Jacquemart for helpful comments about the manuscript.

The research at the Jet Propulsion Laboratory (JPL), California Institute of Technology and College of William and Mary was performed under contract with the National Aeronautics and Space Administration. The research at the University of Massachusetts Lowell was supported by the National Science Foundation through Grant ATM-9415454. This research at PNL was supported by the United States Department of Energy, Office of Basic Energy Sciences, Chemical Sciences Division. The support of CNRS (France)–RFBR(Russia) through the PICS exchange program N2601572 is

acknowledged. Most of the research at the Laboratoire de Physique de l'Université de Bourgogne (LPUB) was supported in the framework of the French Programme National de Chimie Atmosphèrique. Support for the University of Burgundy Physics Laboratory computer equipment from the Region Bourgogne is gratefully acknowledged. Work by Predoi-Cross was supported by the Natural Sciences and Engineering Research Council of Canada, COMDEV, BOMEM Inc, the Meteorological Service of Canada, the University of Toronto Research Fund and the Canadian Space Agency.

References

[1] Burrows A, Hubbard WB, Lunine JI, Liebert J. The theory of brown dwarfs and extrasolar giant planets. Rev Mod Phys 2001;73:719–65.

[2] Brown LR, Margolis JS, Champion JP, Hilico JC, Jouvard JM, Loete M, Chackerian C, Tarrago G, Benner DC. Methane and its isotopes—current status and prospects for improvement. JQSRT 1992;48:617–28.

[3] Rothman LS, Gamache RR, Tipping RH, Rinsland CP, Smith MAH, Benner DC, Devi VM, Flaud JM, Camy-Peyret C, Perrin A, Goldman A, Massie ST, Brown LR, Toth RA. The HITRAN molecular database—editions of 1991 and 1992. JQSRT 1992;48:469–507.

[4] Rothman LS, Rinsland CP, Goldman A, Massie ST, Edwards DP, Flaud JM, Perrin A, Camy-Peyret C, Dana V, Mandin JY, Schroeder J, McCann A, Gamache RR, Wattson RB, Yoshino K, Chance KV, Jucks KW, Brown LR, Nemtchinov V, Varanasi P. The HITRAN molecular spectroscopic database and HAWKS (HITRAN Atmospheric Workstation): 1996 edition. JQSRT 1998;60:665–710.

[5] Rothman LS, Clerbaux C, Dana V, Devi VM, Fayt A, Flaud JM, Gamache RR, Goldman A, Jacquemart D, Jucks KW, Lafferty WJ, Mandin JY, Massie ST, Nemtchinov V, Newnham DA, Perrin A, Rinsland CP, Schroeder J, Smith KM, Smith MAH, Tang K, Toth RA, Vander Auwera J, Varanasi P, Yoshino K. The HITRAN Molecular Spectroscopic Database: edition of 2000 Including Updates through 2001. JQSRT 2003.

[6] Hilico JC, Loete L, Champion JP, Destomes JL, Bogey M. The millimeter-wave spectrum of methane. J Mol Spectrosc 1987;122:381–9.

[7] Oldani M, Bauder A, Hilico JC, Loete M, Champion JP. Microwave Fourier transform spectroscopy of rovibrational transitions in the v_2–v_4 Dyads of $^{12}CH_4$ and $^{13}CH_4$. Europhys Lett 1987;4:29–33.

[8] Roche C, Champion JP. Analysis of dyad–dyad transitions of $^{12}CH_4$ and $^{13}CH_4$. Can J Phys 1991;69:40–51.

[9] Champion JP, Hilico JC, Brown LR. The vibrational ground-state of $^{12}CH_4$ and $^{13}CH_4$. J Mol Spectrosc 1989;133:244–55.

[10] Champion JP, Hilico JC, Wenger C, Brown LR. Analysis of the v_2/v_4 Dyad of $^{12}CH_4$ and $^{13}CH_4$. J Mol Spectrosc 1989;133:256–72.

[11] Brown LR, Loete M, Hilico JC. Linestrengths of the v_2 and v_4 bands of $^{12}CH_4$ and $^{13}CH_4$. J Mol Spectrosc 1989;133:273–311.

[12] Hilico JC, Baronov GS, Bronnikov DK, Gavrikov SA, Nikolaev II, Rusanov VD, Filimonov YG. High-resolution spectroscopy of (pentad–dyad) and (octad–pentad) hot bands of methane in a supersonic jet. J Mol Spectrosc 1993;161:435–44.

[13] Poussigue G, Pascaud E, Champion JP, Pierre G. Rotational analysis of vibrational polyads in tetrahedral molecules—simultaneous analysis of the pentad energy-levels of $^{12}CH_4$. J Mol Spectrosc 1982;93:351–80.

[14] Pierre G, Champion JP, Guelachvili G, Pascaud E, Poussigue G. Rotational analysis of vibrational polyads in tetrahedral molecules—line parameters of the infrared-spectrum of $^{12}CH_4$ in the range 2250–3260 cm^{-1}—theory versus experiment. J Mol Spectrosc 1983;102:344–60.

[15] Toth RA, Brown LR, Hunt RH, Rothman LS. Line parameters of methane from 2385 to 3200 cm^{-1}. Appl Opt 1981;20:932–5.

[16] Brown LR. Methane line parameters from 3700 to 4136 cm^{-1}. Appl Opt 1990;27:3275–9.

[17] Brown LR, Rothman LS. Methane line parameters for the 2.3 − μm region. Appl Opt 1982;21:2425–7.

[18] Margolis JS. Empirical values of the ground-state energies for methane transitions between 5500 and 6150 − cm^{-1}. Appl Opt 1990;29:2295–302.

[19] Margolis JS. Measured line positions and strengths of methane between 5500 and 6180 cm^{-1}. Appl Opt 1988;27:4038–51.
[20] Champion JP, Loete M, Pierre G. in Spectroscopy of the earth, atmosphere and interstellar molecules. New York: Academic Press, 1992. p. 339–422.
[21] Hilico JC, Champion JP, Toumi S, Tyuterev VlG, Tashkun SA. New analysis of the pentad system of methane and prediction of the (pentad–pentad) spectrum. J Mol Spectrosc 1994;168:455–76.
[22] Fejard L, Champion JP, Jouvard JM, Brown LR, Pine AS. The intensities of methane in the 3–5 μm region revisited. J Mol Spectrosc 2000;201:83–94.
[23] Jouvard JM, Lavorel B, Champion JP, Brown LR. Preliminary analysis of the pentad of $^{13}CH_4$ from Raman and infrared spectra. J Mol Spectrosc 1991;150:201–17.
[24] Hilico JC, Robert O, Loete M, Toumi S, Pine AS, Brown LR. Analysis of the interacting octad system of $^{12}CH_4$. J Mol Spectrosc 2001;208:1–13.
[25] Tyuterev VlG, Champion JP, Pierre G, Perevalov VI. Parameters of reduced Hamiltonian and invariant parameters of interacting E and $F2$ fundamentals of tetrahedral molecules. J Mol Spectrosc 1986;120:49–78.
[26] Tyuterev VlG, Champion JP, Pierre G. Reduced effective Hamiltonians for degenerate excited vibrational states of tetrahedral molecules. Application to $2v_2$, $v_2 + v_4$ and $2v_4$ of CH_4. Mol Phys 1990;71:95–1020.
[27] Robert O, Hilico JC, Loete M, Champion JP, Brown LR. First assignment and line strengths of the $4v_4$ band of $^{12}CH_4$ near 1.9 μm. J Mol Spectrosc 2001;209:14–23.
[28] Nikitin A, Champion JP, Tyuterev VlG. Improved algorithms for the modeling of vibrational polyads of polyatomic molecules: application to T_d, O_h, and C_{3v} molecules. J Mol Spectrosc 1998;182:72–84.
[29] Nikitin A, Champion JP, Tyuterev VlG. The MIRS computer package for the modeling of vibration-rotation spectra of polyatomic molecules. JQSRT 2003, in preparation.
[30] Nikitin A, Champion JP, Tyuterev VlG, Brown LR. The high resolution infrared spectrum of CH_3D in the region 900–1700 cm^{-1}. J Mol Spectrosc 1997;184:120–8.
[31] Nikitin A, Champion JP, Tyuterev VlG, Brown LR, Mellau G, Lock M. The infrared spectrum of CH_3D between 900 and 3200 cm^{-1}: extended assignment and modeling. J Mol Struct 2000;517:1–24.
[32] Nikitin A, Brown LR, Fejard L, Champion JP, Tyuterev VlG. Analysis of the CH_3D nonad from 2000–3300 cm^{-1}. J Mol Spectrosc 2002;216:225–51.
[33] Ouardi O, Hilico JC, Loete M, Brown LR. The hot bands of methane between 5 and 10 μm. J Mol Spectrosc 1996;180:311–22.
[34] Tyuterev VlG, Babikov Yu L, Tashkun SA, Perevalov VI, Nikitin A, Champion JP, Hilico JC, Loete M, Pierre CL, Pierre G, Wenger CH. TDS spectroscopic databank for spherical tops. JQSRT, in preparation.
[35] Wenger C, Champion JP. Spherical top data system (STDS) software for the simulation of spherical top spectra. JQSRT 1998;59:471–80.
[36] Ballard J, Johnston WB. Self-broadened widths and absolute strengths of $^{12}CH_4$ lines in the 1310–1370 cm^{-1} region. JQSRT 1986;36:365–71.
[37] Rinsland CP, Malathy Devi V, Smith MAH, Benner DC. Measurements of air-broadened and nitrogen-broadened Lorentz width coefficients and pressure shift coefficients in the v_4 and v_2 bands of $^{12}CH_4$. Appl Opt 1988;27:631–51.
[38] Malathy Devi V, Rinsland CP, Smith MAH, Benner DC. Air-broadened Lorentz halfwidths and pressure-induced line shifts in the v_4 band of $^{13}CH_4$. Appl Opt 1988;27:2296–308.
[39] Smith MAH, Rinsland CP, Devi VM, Benner DC. Temperature-dependence of broadening and shifts of methane lines in the v_4 band. Spectrochim Acta 1992;48A:1257–72.
[40] Devi VM, Benner DC, Smith MAH, Rinsland CP. Measurements of air-broadened, N_2-broadened, and O_2-broadened half-widths and pressure-induced line shifts in the v_3 band of $^{13}CH_4$. Appl Opt 1991;30:287–304.
[41] Pine AS. Self-broadening, N_2-broadening, O_2-broadening, H_2-broadening, Ar-broadening, and He-broadening in the v_3 band Q-branch of CH_4. J Chem Phys 1992;97:773–85.
[42] Benner DC, Devi VM, Smith MAH, Rinsland CP. Air-broadening, N_2-broadening, and O_2-broadening and shift coefficients in the v_3 spectral region of $^{12}CH_4$. JQSRT 1993;50:65–89.
[43] Devi VM, Benner DC, Smith MAH, Rinsland CP. Temperature-dependence of Lorentz air-broadening and pressure-shift coefficients of $^{12}CH_4$ lines in the 2.3 − μm spectral region. JQSRT 1994;51:439–65.

[44] Devi VM, Benner DC, Smith MAH, Rinsland CP. Measurements of air-broadening and pressure-shifting of methane lines in the 2.3 − μm regio. J Mol Spectrosc 1993;157:95–111.
[45] Predoi-Cross A, Devi VM, Benner DC, Brown LR. Self- and air-broadening and shifting of methane in the 4200 –4500 cm^{-1} spectral range. The 57th Symposium on Molecular Spectroscopy, Ohio State University, 2003 and paper in preparation.
[46] Devi VM, Benner DC, Smith MAH, Rinsland CP. Measurements of air broadening, pressure shifting and off diagonal relaxation matrix coefficients in the v_3 band of $^{12}CH_3D$. J Mol Struct 2000;517:455–75.
[47] Devi VM, Benner DC, Smith MAH, Rinsland CP. Measurements of air broadened width and air induced shift coefficients and line mixing in the v_5 band of $^{12}CH_3D$. JQSRT 2001;68:135–61.
[48] Devi VM, Benner DC, Smith MAH, Rinsland CP, Brown LR. Measurements of air-broadened width and air-induced shift coefficients and line mixing in the v_6 band of $^{12}CH_3D$. JQSRT 2001;68:1–41.
[49] Devi VM, Benner DC, Brown LR, Smith MAH, Rinsland CP, Sams RL, Sharpe SW. Multi-spectrum analysis of self- and N_2-broadening, shifting and line mixing coefficients in the v_6 band of $^{12}CH_3D$. JQSRT 2002;72:139–91.
[50] Devi VM, Benner DC, Smith MAH, Rinsland CP, Brown LR. Multispectrum analysis of self- and nitrogen-broadening, pressure shifting and line mixing in the v_3 parallel band of $^{12}CH_3D$. JQSRT 2002;73:603–40.
[51] Devi VM, Benner DC, Smith MAH, Rinsland CP, Brown LR. Self- and N_2-broadening, pressure induced shift and line mixing in the v_5 band of $^{12}CH_3D$ using a multi-spectrum fitting technique. JQSRT 2002;74:1–41.
[52] Benner DC, Devi VM, Smith MAH. unpublished data.
[53] Tarrago G, Delaveau M, Fusina L, Guelachvili G. Absorption of $^{12}CH_3D$ at 6–10 μm: triad v_6, v_3, v_5. J Mol Spectrosc 1988;12:149–58.
[54] Ulenikov ON, Onopenko GA, Tyabaeva NE, Anttila R, Alanko S, Schroderus J. Study on the rovibrational interactions and a_1/a_2 splittings in the v_6, v_3, v_5 triad of CH_3D. J Mol Spectrosc 2000;200:1–15.
[55] Brown LR, Nikitin A, Devi VM, Benner DC, Smith MAH, Fejard L, Champion JP, Tyuterev VlG. Line intensities of CH_3D in the triad region: 6–10 μm, in preparation.
[56] Ulenikov ON, Onopenko GA, Tyabaeva NE, Anttila R, Alanko S, Schroderus J. Rotational analysis of the ground state and the lowest fundamentals v_3, v_5, v_6 of $^{13}CH_3D$. J Mol Spectrosc 2000;201:9–17.
[57] Rothman LS, Gamache RR, Goldman A, Brown LR, Toth RA, Pickett HM, Poynter RL, Flaud J-M, Camy-Peyret C, Barbe A, Husson N, Rinsland CP, Smith MAH. The HITRAN database—1986 edition. Appl Opt 1987;26:4058 –97.
[58] Drummond JR, Mand GS. The measurements of pollution in the troposphere (MOPITT) instrument: overall performance and calibration requirements. J Atmos Ocean Tech 1996;13:314–20.
[59] Strong K, Taylor FW, Calcutt SB, Remedios JJ, Ballard J. Spectral parameters of self-broadened and hydrogen-broadened methane from 2000 cm^{-1} to 9500 cm^{-1} for remote sounding of the atmosphere of Jupiter. JQSRT 1993;50:363–429.
[60] Baines KH, West RA, Giver LP, Moreno F. Quasi-random narrow-band model fits to near-infrared low-temperature laboratory methane spectra and derived exponential sum absorption-coefficients. J Geophys Res Planet 1993;98:5517 –29.
[61] O'Brien JJ, Cao H. Absorption spectra and absorption coefficients for methane in the 750–940 nm region obtained by intracavity laser spectroscopy. JQSRT 2002;75:323–50.
[62] Brown LR. Near-IR linelist of methane positions and intensities at room temperature, in preparation.
[63] Hippler M, Quack M. High-resolution Fourier transform infrared and cw-diode laser cavity ringdown spectroscopy of the $v_2 + 2v_3$ band of methane near 7510 cm^{-1} in slit jet expansions and at room temperature. J Chem Phys 2002;116:6045–55.
[64] Pierre G, Hilico JC, Debergh C, Maillard JP. The region of the v_3 band of methane. J Mol Spectrosc 1980;82:379 –93.
[65] Nasser R, Bernath PF. Combining Laboratory Hot Methane Spectra with HITRAN for Astrophysical Applications. JQSRT, this issue.
[66] Venuti E, Halonoen L, Della Valle RG. High dimensional anharmonic potential energy surfaces: the case of methane. J Chem Phys 1999;110:7339–47.
[67] Schwenke DW. Towards accurate ab initio predictions of the vibrational spectrum of methane. Spectrochim Acta A 2002;58:849–91.

[68] Borysow A, Champion JP, Jorensen UG, Wenger C. Towards simulation of high temperature methane spectra. Mol Phys 2002;100:3585–94.
[69] Wishnow EH, Gush HP, Halpern M, Ozier I. In: Salama F, editior. NASA Conference Proceedings for the NASA Laboratory Astrophysics workshop, Ames Research Center, 2003, in press.
[70] Brown LR, Toth RA, Dulick M. Empirical line parameters of $^{16}H_2O$ near 0.94 μm: positions, intensities and air-broadening coefficients. J Mol Spectrosc 2002;212:57–82.
[71] Pieroni D, Hartmann J-M, Camy-Peyret C, Jeseck P, Payan S. Influence of line mixing on absorption by CH_4 in atmospheric balloon-borne spectra near 3.3 μm. JQSRT 2001;68:117–33.
[72] Dicke RH. The effect of collisions upon the Doppler width of spectral lines. Phys Rev 1953;89:472.
[73] Wittke JP, Dicke RH. Redetermination of the hyperfine splitting in the ground state of atomic hydrogen. Phys Rev 1956;103:620–31.
[74] Galatry L. Simultaneous effect of Doppler and foreign gas broadening on spectral lines. Phys Rev 1961;122:1218–23.
[75] Rautian SG, Sobel'man II. The effect of collisions on the Doppler broadening of spectral lines. Simultaneous effect of Doppler and foreign gas broadening on spectral lines. Sov Phys Uspekhi 1967;9:701–16.
[76] Berman PR. Speed-dependent collisional width and shift parameters in spectral profiles. JQSRT 1972;12:1331–42.
[77] Ward J, Cooper J, Smith EW. Correlation effects in theory of combined Doppler and pressure broadening 1 Classical theory. JQSRT 1974;14:555–90.
[78] Baranger M. Problem of overlapping lines in the theory of pressure broadening. Phys Rev 1958;111:494–504.
[79] Kolb AC, Griem H. Theory of line broadening in multiplet spectra. Phys Rev 1958;111:514–21.
[80] Fano U. Pressure broadening as a prototype of relaxation. Phys Rev 1963;131:259–68.
[81] Ben-Reuven A. Impact broadening of microwave spectra. Phys Rev 1966;145:7–22.
[82] Gordon RG, McGinnis RP. Intermolecular potentials and infrared spectra. J Chem Phys 1971;55:4898–906.
[83] Rosenkranz PW. Shape of 5 mm oxygen band in atmosphere. IEEE Trans Antennas Prop 1975;AP-23:498–506.
[84] Ciurylo R, Szudy J. Speed-dependent pressure broadening and shift in the soft collision approximation. JQSRT 1997;57:411–23.
[85] Lance B, Blanquet G, Walrand J, Bouanich JP. On the speed-dependent hard collision lineshape models: application to C_2H_2 perturbed by Xe. J Mol Spectrosc 1997;185:262–71.
[86] Lance B, Robert D. An analytical model for collisional effects on spectral line shape from the Doppler to the collision regime. J Chem Phys 1998;109:8283–8.
[87] Ciurylo R, Pine AS, Szudy J. A generalized speed-dependent line profile combining soft and hard partially correlated Dicke-narrowing collisions. JQSRT 2001;68:257–71.
[88] Ciurylo R, Jaworski R, Jurkowski J, Pine AS, Szudy J. Spectral line shapes modeled by a quadratic speed-dependent Galatry profile. Phys Rev A 2001;63:032507–17.
[89] Pine AS. Line mixing sum rules for the analysis of multiplet spectra. JQSRT 1997;57:145–55.
[90] Ciurylo R, Pine AS. Speed-dependent line mixing profiles. JQSRT 2000;67:375–93.
[91] Benner DC, Rinsland CP, Devi VM, Smith MAH, Atkins D. A multispectrum nonlinear least-squares fitting technique. JQSRT 1995;53:705–21.
[92] Pine AS. N_2 and Ar broadening and line mixing in the P and R branches of the ν_3 band of CH_4. JQSRT 1997;57:157–76.
[93] Pieroni D, Nguyen-Van-Thanh, Brodbeck C, Claveau C, Hartmann JM, Gabard T, Champion JP, Bermejo D, Domenech JL, Claveau C, Valentin A. Experimental and theoretical study of line mixing in methane spectra I The N_2-broadened ν_3 band at room temperature. J Chem Phys 1999;110:7717–32.
[94] Pine AS, Gabard T. Speed-dependent broadening and line mixing in CH_4 perturbed by Ar and N_2 from multispectrum fits. JQSRT 2000;66:69–92.
[95] Pine AS, Gabard T. Multispectrum fits for line mixing in the ν_3 band Q branch of methane. J Mol Spectrosc 2003, in press.
[96] Neshyba SP, Lynch R, Gamache R, Gabard T, Champion JP. Pressure-induced widths and shifts for the ν_3 band of methane. J Chem Phys 1994;101:9412–21.
[97] Flaud J-M. concerning MIPAS, private communications.
[98] Toon G. concerning ground-based observations, private communications.